CubeSat Formation Antenna Array Synchronization for GNSS-R

Laurent Paucot*, Eliott Hubin*, Maxime Drouguet*, Volodymyr Kudriashov†, Jan Thoemel‡, Christophe Craeye*
*ICTEAM/ELEN, Université catholique de Louvain, Louvain-la-Neuve, Belgium, laurent.paucot@uclouvain.be
†ESTEC, ESA, Netherlands
‡Interdisciplinary Centre for Reliability, Security and Trust (SnT), University of Luxembourg, Luxembourg-ville, Luxembourg, jan.thoemel@uni.lu

***Abstract*—This paper presents an approach to improving GNSS-R Earth observation resolution. The proposed method involves using a large antenna array comprising CubeSats flying in formation to synthetically increase the aperture. The paper discusses how the orbital constraints necessitate changes to the formation over time and require the formation plane to be inclined relative to the Earth's surface. The study examines a 1 km resolution target, side lobe level restrictions, and the isotropy of the ground spot. Synchronization challenges are explored by characterizing an antenna array involving CubeSat prototypes.**

***Index Terms*—GNSS-R, CubeSat, synchronization, beamforming, orbital constraint.**

I. Introduction

Earth observation is among the most rewarding applications in spaceflight. Initially important for defence purposes, it is today employed for many uses such as the remote sensing of the effects of climate change. Imagery and elaborate data products are commercially available. However new Earth observation techniques are still found with the potential to respond to open scientific questions. Among those is the so-called Global Navigation Satellite System-reflectometry (GNSS-R) method, that is, the acquisition and use of GNSS-transmitted signals after their reflection off the Earth's surface.

The theory of GNSS-R has been developped in 1988 for scatterometry [1] and in 1993 for altimetry [2]. The former can be performed based on the peak power as well as from the widening of the waveform of the scattered GNSS signal. In essence the method samples data on the surface permittivity. The signal is impacted by the surface roughness. Either information can be used to probe the surface. For instance, water content of soil or wave-induced ocean roughness allowing one to derive wind-speed near the specular point can be sensed. Altimetry is based on time-of-flight difference. It can be used to detect ice sheet presence and thickness in the Arctic.

The technology has first been demonstrated in [3] from a Low Earth Orbit (LEO). In essence, it is an L-band bistatic radar application, as the transmitter and receiver of the radio signal are separated. It is thus cost-effective and independent from illumination and weather conditions, which are challenges for most other Earth observation methods. However, the resolution is poor compared to imaging or radar techniques. We research how to further improve the GNSS-R technology by adding an interferometric component. We suggest that CubeSats may be a suitable platform for this measurement technique as it requires only modest satellite system resources. The miniaturization, use of the mature and modular platform and economic launch opportunities enable a low-cost mission or an increased data return for a given budget.

In particular, we investigate how the resolution of the system can be improved. An apparent option would be to increase the aperture size. The beamwidth is indeed proportional to λ/L with λ and L respectively referring to the wavelength and the characteristic length of the antenna. Beamforming for GNSS-R has been studied in the framework of the GEROS-ISS project [4]. However the proposed antenna array is limited to a one-metre square payload mounted on the International Space Station (ISS). Because the increase of the antenna size would be excessive, one should rather employ a distributed antenna array of which elements are placed on several satellites flying in proximity, that is, in a formation. This at the same time provides the opportunity to form and shape an equivalent beam allowing one to improve the resolution. The idea is illustrated in Fig. 1. The paper is organized as follows. Section II covers the orbital constraints associated with CubeSat flights. In Section III, we present an array configuration and its associated radiation pattern and ground spot. Section IV includes an analysis of a first prototype that addresses the synchronization challenge, and Section V concludes the paper.

II. Orbital constraints

In the proposed concept, the beamforming GNSS-R method would be employed on several CubeSats orbiting the Earth in a circular Low Earth Orbit (LEO). Orbital mechanics dictate that not every formation geometry is possible. For instance, a satellite can not fly above another one. The different altitudes would imply different orbital speeds and the drifting apart of the satellites. Physically accepted geometries are those satisfying the Clohessy-Wiltshire (CW) equations governing formation flight [5]. So far, circular configurations are promising [6]. Perturbations require that the formation geometry is maintained for instance through propulsive means [7] or through the use of aerodynamic forces [8]–[10].

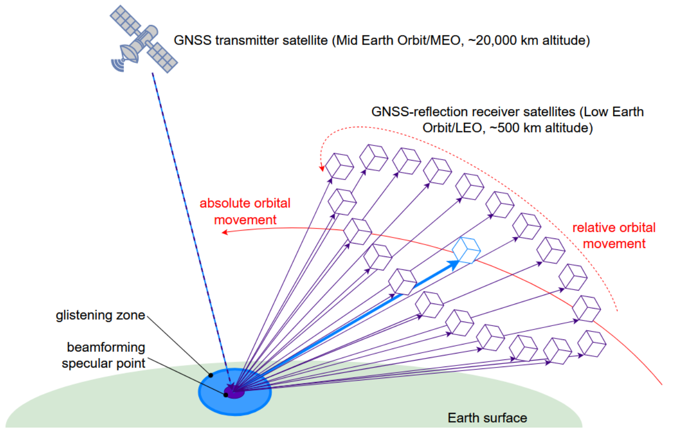

Fig. 1. The GNSS-reflectometry Earth observation method using one satellite or a formation thereof (not to scale).

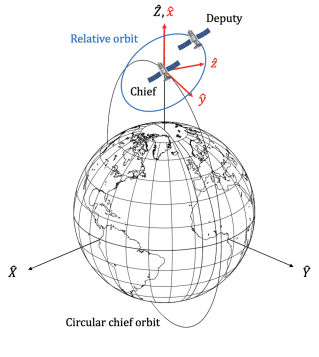

Fig. 2. Absolute ($\hat{X}$, $\hat{Y}$, $\hat{Z}$) and relative ($\hat{x}$, $\hat{y}$, $\hat{z}$) systems of coordinates.

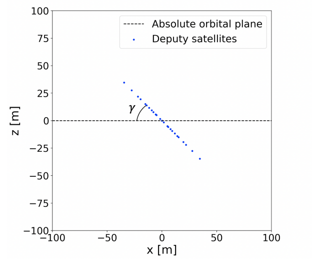

Fig. 3. γ = 45 deg. tilt of the formation with respect to the absolute orbital plane, no alteration in the overall shape.

A. *Temporal evolution*

One primary orbital constraint for Earth observation using an antenna array mounted on CubeSats is the dynamic nature of a formation. The CW equations assume a slight ellipticity in the absolute orbits of each secondary satellite around the chief one. Consequently, this ellipticity introduces variations in angular rotation speeds, leading to an evolving, non-static configuration. This variation becomes evident when representing the relative motion of a formation over a complete period, where the shape of the relative orbits clearly exhibits a strong elliptical configuration.

B. *Formation tilt*

In its simplest way, the CW equations enable a relative movement in the absolute orbital plane as for instance an ellipse in the $\hat{x}$-$\hat{y}$ plane (see Fig. 2), i.e. perpendicular to the Earth surface. Such geometry would not suite the beamforming Earth observation method and thus a motion into the $\hat{z}$-direction, i.e. out-of-the-orbital plane, is needed.

This motion permits a tilt of the formation plane (around the $\hat{y}$-axis) of 45 deg. with respect to the absolute orbital plane of the chief circular orbit (see Fig. 3) without altering the general shape of the formation. However, any further increase in the inclination angle inevitably results in the elongation of the formation along its minor axis. A similar effect can be observed when the inclination angle decreases, causing the formation to compress along its minor axis. In other terms, a higher (or lower) tilt of the formation plane relative to the absolute orbital plane of the chief satellite results in a more pronounced stretching (or compression) of the formation along its minor axis. Consequently, maintaining such a formation in a plane locally parallel to the surface of the Earth becomes unattainable, unless the minor axis is infinitely stretched.

III. Array configurations

A. *Objectives*

The purpose is to design an (irregular) antenna layout that is sufficiently directive to achieve high resolution on Earth, while limiting the level of side lobes directed toward the glistening zone. The existence of side lobes in this area may introduce unwanted interference from outside the observed spot on the Earth.

The following quantitative objectives have been formulated. Knowing that,

- the antenna array will be orbiting at about 400 km above the Earth surface,
- the glistening zone is defined as a disk with an approximate 10 km diameter and
- the number of elements shall not exceed 32 elements for cost reasons,

the following specifications should be reached :

- an illumination spot of maximum 1 km diameter within the glistening zone and
- side lobes of the array factor limited to -13.3 dB inside the glistening zone (typical side lobe level in a uniform square aperture).

There are no restrictions on side lobes outside the glistening zone. For antenna design, a CubeSat requires a minimum altitude of 400 km in Low Earth Orbit (LEO), as specified in [11]. The size of the glistening zone (10 km), as determined in [12], corresponds to the highest level of accuracy achievable in extreme conditions, such as those found in very mountainous regions. Regarding the resolution, the aim is to increase what currently exists by a factor of 10. For instance, the CYGNSS mission has a resolution of 10-25 km depending on contexts [13], [14]. Higher resolution has been announced in [15], but it concerns only coherent scattering.

B. *Space tapering*

A common approach when trying to achieve a given beamwidth and side lobe levels is to synthesize non-regular planar arrays to approximate the radiation pattern of a continuous aperture that would have the same radius as the array [16]. This method, known as space tapering, can be thought of as the spatial sampling of a continuous aperture.

An estimate of the main beam width for a homogeneously and densely sampled aperture, also proposed in [16], is $\sin\alpha \approx \lambda/2R$ with R the radius of the equivalent continuous aperture. Recalling the 1 km resolution expected, this gives

$R \approx 80$ m, knowing that $\lambda = 0.2$ m (L1 band). Therefore, the antenna array should sample a disk of 80 m radius, with uniform density being ideal.

C. Radiation pattern

It is assumed that the CubeSats will carry identical antennas with a unitary complex amplitude and an isotropic element pattern. The validity of the latter hypothesis is dependent on studying the radiation pattern within a limited region, typically the order of magnitude of the glistening zone, around the main beam. It has been demonstrated in [17] that the CubeSat's element pattern is sufficiently large in the nadir direction: authors specifically show a simple way to exploit scattering by the satellite to achieve low backlobes. Consequently, the radiation pattern and array factor will be considered equivalent here.

So far, promising results have been achieved through the precise arrangement of four-arm (each composed of 7 elements) spiral antennas to which the chief satellite should be added (see Fig. 4). The formation is thus made of 29 elements. Space tapering by means of spiral formation has already been studied and demonstrated good results in reducing side lobe levels [16], [18]. The positioning of each antenna adheres to the physical principles outlined in the CW equations, where 7 concentric relatives orbits are arranged to form this spiral-shaped configuration. Each of these relative orbit exhibits a strong elliptical shape (cf. Section II-A) which directly depends on the orbital inclination. The outermost orbit has a semi-major axis length of 70 m, which is close to the 80 m radius estimated in Section III-B, while the semi-minor axis follows the physics of CW by having half of the semi-major axis size. Fig. 5 shows that this configuration provides a resolution of 0.94 km, while ensuring that secondary lobes remain below -12.5 dB in the glistening zone. The resolution requirement is satisfied and the level of side lobes is within 1 dB of the -13.3 dB target. This pattern corresponds to the nadir observation from the spiral obtained in the $\hat{x}$-$\hat{y}$ plane and positioned in the $\hat{z}$-$\hat{y}$ plane. It would correspond to an ideal situation where the tilt would not influence the formation.

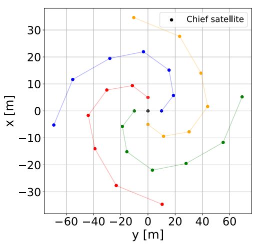

Fig. 4. 4-arms of 7 elements spiral formation.

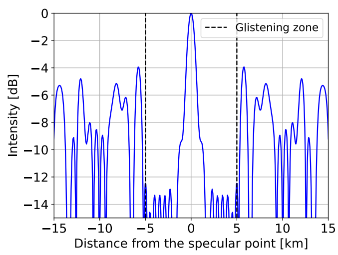

Fig. 5. Nadir observation radiation pattern of the 4-arms spiral formation (ideal situation).

D. Ground spot

The ground spot (projection of the power distribution radiated onto the Earth's surface) is used to highlight the footprint produced by the main beam and analyze its evolution based on various factors such as the formation flight, number of satellites within a constellation, inclination of the formation plane, the position of the GNSS satellite, and the relative motions of concentric circles.

This analysis showed that the inclination of the satellite plane, initially regarded as a constraint, ultimately may be a contributing factor in maintaining a sufficiently isotropic directive beam. The desire to uphold such an isotropic beam is driven by the necessity for Earth observation resolution to remain as consistent as possible.

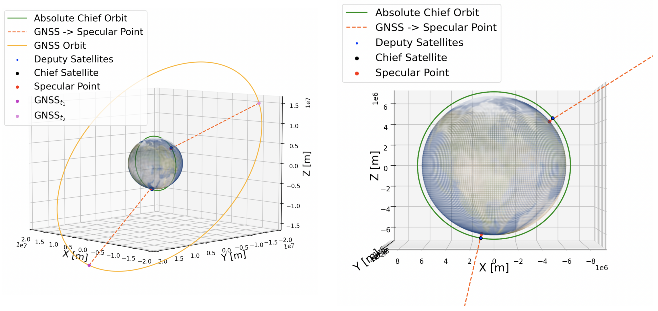

Fig. 6. Positioning of the spiral configuration (illustrated in Fig. 4) at two different and arbitrary locations around the Earth, at 1/5 and 3/5 of the orbital period.

Through the examination of various positions of the CubeSat formation around the Earth, an interesting result emerges: despite the evolution of the overall shape of the formation over time and the position of the specular point, a judicious inclination of the CubeSats' plane allows most of the time the preservation of a completely circular main beam and, by extension, an isotropic resolution (see Fig. 7). Issues may arise when the specular point appears in a direction opposite to that towards which the formation is inclined.

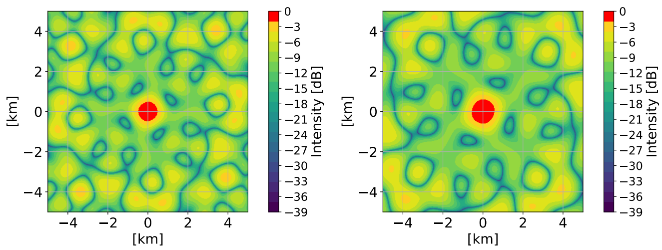

Fig. 7. Ground illumination of the signal received by the CubeSats formation at 1/5 and 3/5 of the orbital period. The formation is tilted at 66.5 deg. and 52.5 deg. around the $\hat{y}$-axis (Section II-B) and at 25 deg. and 20 deg. around the $\hat{z}$-axis, respectively, with respect to the absolute orbital plane. The red disk, symbolizing the illumination of the main beam, appears completely circular, ensuring a sufficiently isotropic resolution.

Note that the various inclinations required to maintain a consistently isotropic spot have an impact on the height of sidelobes in the glistening zone. As a result, some side lobes may exceed -10 dB. However, it is noteworthy that, for the proposed tests, within a 4 km radius, the height of the side lobes meets the specified requirements.

IV. Synchronization

A. Motivation

The scattering of the GNSS signal on the Earth's surface leads to a glistening zone around the specular point, resulting in the reflection of multiple signals that the passive radar, (*i.e.*, the array composed of the CubeSats) receives. The separation of the reflected signals from different zones through digital beamforming enables the formation of an image of the observed area. As a first step, we will demonstrate the ability of a small array of two CubeSat prototypes to carry out direction finding using the MUSIC beamforming algorithm as described in [19] and to satisfy CubeSat synchronization constraints.

B. Constraints

When carrying out beamforming, baseband down-conversion is performed. This requires the use of a single local oscillator (LO), which is then distributed (typically through transmission lines) to each element of the array. However, when the elements are located on several CubeSats, wired transmission of the LO is no longer possible. More specifically, we aim to develop a solution that allows us to perform regular beamforming under the following constraints:

- Wireless transmission of the LO
- Element spacing variation

The second limitation is imposed by the orbital flight, as already explained in Section II. This entails a synchronization challenge due to the phase shifts induced on the local oscillator tone by differences in propagation time.

C. Solution

Phase synchronization techniques in distributed systems have been discussed in previous publications [20], [21]. The authors of [20], present a technique that utilizes an external beacon, which could be placed on a geostationary spacecraft, to trigger data transmission to a ground receiver. The main drawbacks of this approach are the requirement to launch an additional spacecraft that will not participate in beamforming, as well as launching to a much higher orbit than the formation of CubeSats.

The solution proposed here consists of a chief CubeSat that broadcasts a reference tone (RT) to the deputy CubeSats, responsible of rebuilding a coherent local oscillator.

An anechoic chamber has been used to characterize an array made of two CubeSat prototypes (see Fig. 8) for the purpose of implementing single-source localization via the MUSIC digital beamforming algorithm. This basic experiment demonstrates the proper reference tone (RT) transfer allowing phase synchronization. It should be noted that the MUSIC algorithm was developed to perform multiple source separation and that a mathematical equivalence with regular digital beamforming can be demonstrated in the case of single-source localization [22]. In this prototype, the GNSS signal reflection is replicated

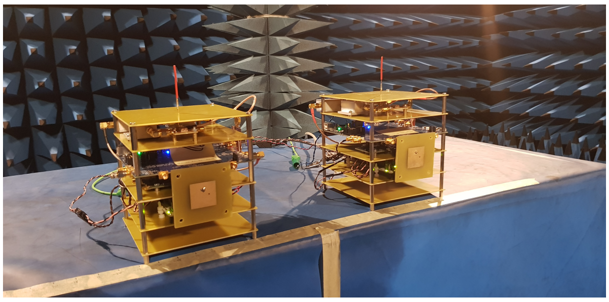

Fig. 8. Array of CubeSat prototypes with (red) monopoles for receiving the RT and patch antennas for the 2.4 GHz simulated GNSS reflected signal.

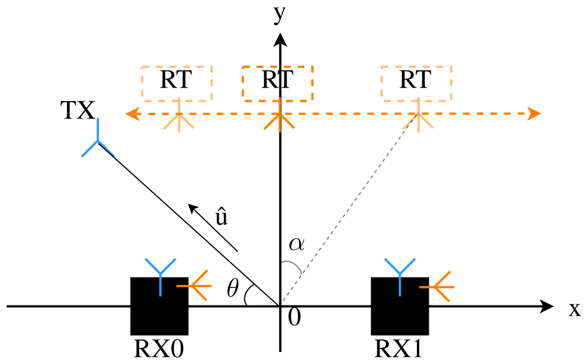

Fig. 9. Anechoic chamber setup with CubeSats RX0 (x = -0.15 m) and RX1 (x = 0.15 m), 2.4 GHz source TX (θ = 50 deg.) and reference tone RT (constant y = 2.1 m).

by a 2.4 GHz tone (λ = 12 cm), the reference tone is broadcast at 1.2 GHz (λ = 24 cm), while the frequency multiplier present on both CubeSats performs the conversion. The high frequency tone is fine tuned a few kHz above 2.4 GHz in order to obtain a residual intermediate frequency after mixing.

In this configuration (see Fig. 9), the target TX and the CubeSats (RX0 and RX1) remain in a fixed and known position. The reference tone (RT) emitter is moved along a line parallel to the array at known positions. Consequently, the phase shift caused by the displacement of the RT can be theoretically calculated and corrected during post-processing. It should be noted that, as the phase shift depends on the working frequency, a factor 2 (corresponding to 2.4/1.2) needs to be taken into account in the correction.

D. Preliminary results

Fig. 10 shows the absolute error in estimating the direction of arrival (DoA) of the 2.4 GHz source for various positions of the RT. The system was calibrated using the RT placed at x = 0 (α = 0 deg. direction) in Fig. 9, resulting in a zero error at this point. The green curve represents the theoretical DoA estimation without applying any phase shift correction, i.e. the absolute value of α. The orange curve shows the experimental DoA estimation without applying any phase shift correction. The DoA estimation error acquired after the correction of phase shifts is presented in blue. It can be observed that the blue curve is, as expected, the absolute value of the difference

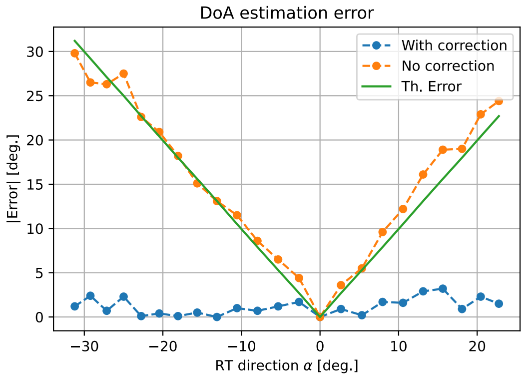

Fig. 10. Theoretical and experimental (one trial) DoA estimation error for α angles (RT direction) between -30 deg. and 20 deg.

between the orange curve and the green curve. The average error (including phase shift correction) is equal to 1.2 deg.

Deviations from the theoretical error are assumed to come from various sources, including residual reflections in the chamber or scattering on CubeSats resulting in an element pattern with a non-constant phase diagram in the horizontal plane that could be corrected by a digital twin.

V. Conclusion

This paper presented a new system for performing GNSS-R Earth observation, namely the use of a synchronized CubeSat formation. We first introduced the orbital constraints imposed by the physics of the CW equations on the CubeSat flight. These constraints are linked to the dynamic nature of formations over an orbital period and their inclination with respect to the absolute orbital plane. Then, we demonstrated how we could achieve a 1 km resolution while limiting the level of the side lobes near the specular point by synthesizing a non-regular planar array in a 4-arm spiral formation. We have demonstrated that although the formation plane is inclined (and not parallel to the surface of the Earth), it is typically feasible to maintain isotropy of the ground spot. Finally, synchronization challenges were highlighted and the characterization of a first array consisting of two CubeSat prototypes was proposed. So far, we are able to perform DoA estimation with a 1.2 deg. average error.

Acknowledgment

The authors are grateful to Dr. Martin-Neira from ESA for drawing their attention to the Scala et al. paper on dynamic satellite formation. The authors also thank the Space4Relaunch program (WP1) funded by Région Wallonne.

References

[1] C. D. Hall and R. A. Cordey, “Multistatic scatterometry,” *Remote sensing. Proc. IGARSS ’88 symposium, Edinburgh, 1988. Vol. 1*, pp. 561–562, 1988.

[2] M. Martin-Neira, “A passive reflectometry and interferometry system (PARIS): application to ocean altimetry,” *ESA Journal*, vol. 17, no. 4, pp. 331–355, 1993.

[3] M. Clarizia, C. Gommenginger, S. Gleason, C. Galdi, and M. Unwin, “Global navigation satellite system-reflectometry (gnss-r) from the uk-dmc satellite for remote sensing of the ocean surface,” in *IGARSS 2008 - 2008 IEEE Int. Geosci. Remote Sens. Symp.*, vol. 1, 2008, pp. I–276–I–279.

[4] J. Wickert, E. Cardellach, M. Martín-Neira, J. Bandeiras, L. Bertino, O. B. Andersen *et al.*, “Geros-iss: Gnss reflectometry, radio occultation, and scatterometry onboard the international space station,” *IEEE J. Sel. Topics Appl. Earth Observ. Remote Sens.*, vol. 9, no. 10, pp. 4552–4581, 2016.

[5] W. Clohessy and R. Wiltshire, “Terminal guidance system for satellite rendezvous,” *Journal of the aerospace sciences*, vol. 27, no. 9, pp. 653–658, 1960.

[6] F. Scala, C. Colombo, B. Duesmann, M. Martin-Neira *et al.*, “Analysis and design of future multiple satellite formation flying L-band missions in Low Earth orbit,” *Proceedings of the International Astronautical Congress 2022*, vol. 2022-September, pp. 1–12, 2022.

[7] O. Montenbruck, R. Kahle, S. D’amico, and J. S. Ardaens, “Navigation and control of the TanDEM-X formation,” *Journal of the Astronautical Sciences*, vol. 56, no. 3, pp. 341–357, 2008.

[8] D. Ivanov, M. Mogilevsky, U. Monakhova, M. Ovchinnikov, and A. Chernyshov, “Deployment and maintenance of nanosatellite tetrahedral formation flying using aerodynamic forces,” *Proceedings of the International Astronautical Congress, IAC*, vol. 2018-October, no. October, p. 11, 2018.

[9] C. Traub, F. Romano, T. Binder, A. Boxberger, G. H. Herdrich, S. Fasoulas *et al.*, “On the exploitation of differential aerodynamic lift and drag as a means to control satellite formation flight,” *CEAS Space Journal*, vol. 12, no. 1, pp. 15–32, 2020.

[10] J. Thoemel and T. van Dam, “Autonomous formation flight using solar radiation pressure,” *CEAS Space Journal*, vol. 13, no. 4, pp. 555–566, 2021.

[11] S. Liu, P. I. Theoharis, R. Raad, F. Tubbal, A. Theoharis, S. Iranmanesh *et al.*, “A survey on cubesat missions and their antenna designs,” *Electronics*, vol. 11, no. 13, 2022.

[12] U.-P. Duraffourd, “Cubesats in formation for earth observation,” Master’s thesis, Ecole polytechnique de Louvain, Université catholique de Louvain, 2022, Adv. : Craeye, Christophe ; Fisette, Paul.

[13] F. Lei, V. Senyurek, M. Kurum, A. Gurbuz, D. Boyd, and R. Moorhead, “Quasi-global gnss-r soil moisture retrievals at high spatio-temporal resolution from cygnss and smap data,” in *2021 IEEE Int. Geosci. Remote Sens. Symp. IGARSS*, 2021, pp. 6303–6306.

[14] S. Gleason, C. S. Ruf, M. P. Clarizia, and A. J. O’Brien, “Calibration and unwrapping of the normalized scattering cross section for the cyclone global navigation satellite system,” *IEEE Trans. Geosci. Remote Sens.*, vol. 54, no. 5, pp. 2495–2509, 2016.

[15] S. Gleason, A. O’Brien, A. Russel, M. M. Al-Khaldi, and J. T. Johnson, “Geolocation, calibration and surface resolution of cygnss gnss-r land observations,” *Remote Sensing*, vol. 12, no. 8, 2020.

[16] T. Clavier, N. Razavi-Ghods, F. Glineur, D. González-Ovejero, E. de Lera Acedo, C. Craeye, and P. Alexander, “A global-local synthesis approach for large non-regular arrays,” *IEEE Trans. Antennas Propag.*, vol. 62, no. 4, pp. 1596–1606, 2014.

[17] V. Sokolow, F. Jabbarigargari, P. Fisette, and C. Craeye, “Scanning GNSS-R beams from cubesats using sequentially rotated deployable dipoles,” in *2021 IEEE Int. Geosci. Remote Sens. Symp. IGARSS*, 2021, pp. 8538–8541.

[18] M. Viganó, G. Toso, C. Gerard, M. Cyril, and I. Lager, “Sunflower array antenna with adjustable density taper,” *Int. Journal of Antennas and Propagat.*, vol. 2009, 01 2009.

[19] R. Schmidt, “Multiple emitter location and signal parameter estimation,” *IEEE Trans. Antennas Propag.*, vol. 34, no. 3, pp. 276–280, 1986.

[20] P. Sundaramoorthy, E. Gill, and C. Verhoeven, “Beamforming with spacecraft under reduced localization and clock constraints,” *IEEE Transactions on Aerospace and Electronic Systems*, vol. 52, no. 3, pp. 1197–1209, 2016.

[21] D. Jenn, Y. Loke, M. Tong, E. C. Yeo, and R. Broadston, “Distributed phased arrays with wireless beamforming,” in *2007 Conference Record of the Forty-First Asilomar Conference on Signals, Systems and Computers*, 2007, pp. 948–952.

[22] G. Hislop and C. Craeye, “On the mathematical link between the music algorithm and interferometric imaging,” *IEEE Trans. Antennas Propag.*, vol. 59, no. 4, pp. 1412–1414, 2011.